University of Toronto

Interferometry

Amir Koutahi, Enxi Huang

PHY294
April 18, 2026

Abstract

A Michelson interferometer was used to investigate optical interference phenomena and measure several physical quantities through fringe-counting techniques. The wavelength of a green laser was determined from controlled mirror displacements, and the index of refraction of a plastic sample was obtained using small-angle rotations. The interferometer was also employed to measure the linear thermal expansion coefficient of an aluminum rod by observing fringe shifts caused by temperature changes. Linear least-squares analysis was applied to all measurements, yielding results consistent with accepted values within experimental uncertainty.

Contents

1 Introduction **1**

2 Materials and Methods **1**
2.1 Apparatus Description 1
2.2 Experimental Procedure 2

3 Data and Analysis **3**
3.1 Wavelengths and Coherence Lengths 3
3.2 Index of Refraction 4
3.3 Thermal Expansion of Aluminum 5

4 Discussion and Conclusion **6**

5 References **7**

1 Introduction

Interferometry is an experimental technique that exploits the interference of coherent light to make precise measurements of optical path length differences. By comparing the relative phase of light beams that travel along different paths, interferometers can resolve displacements much smaller than the wavelength of light. In this experiment, a Michelson interferometer is used, which operates by dividing the amplitude of an incident beam into two paths that are reflected by mirrors and recombined to produce an interference pattern.

When one mirror in the interferometer is displaced by a distance Δx, the optical path length changes by $2\Delta x$ due to the round-trip of the light. Each change in path length equal to one wavelength λ causes one interference fringe to appear or disappear, giving the relation

$$N\lambda = 2\Delta x, \tag{1}$$

where N is the number of fringes counted. This relationship allows the wavelength of a light source to be determined from measured mirror displacements.

The interferometer can also be used to measure material properties. When a transparent material of thickness t and index of refraction n is inserted into one arm and rotated by a small angle θ (in radians), the number of fringes observed is approximately

$$N \simeq \frac{t}{\lambda}\theta^2\left(1 - \frac{1}{n}\right). \tag{2}$$

By fitting N as a function of θ^2, the index of refraction of the material can be extracted.

Additionally, thermal expansion of a metal rod placed in one arm of the interferometer causes a change in optical path length. For small temperature changes ΔT, the resulting fringe shift is given by

$$N \simeq \frac{2L_0}{\lambda}\alpha\Delta T, \tag{3}$$

where L_0 is the initial length of the rod and α is its linear thermal expansion coefficient.

The purpose of this experiment is to use a Michelson interferometer to measure the wavelength of a green laser and a red LED, determine the index of refraction of a plastic sample, and measure the thermal expansion coefficient of aluminum through precise fringe-counting techniques.

2 Materials and Methods

2.1 Apparatus Description

The experiment was performed using a Michelson interferometer configured for optical interferometry, as shown schematically in Figure 1. The apparatus consists of a coherent light source, beam-splitting optics, two reflecting arms, and a detection screen.

Light from a green laser source is first expanded and collimated using a converging lens before reaching a front-surface beam splitter. The beam splitter divides the incident beam into two paths of approximately equal intensity. One beam is transmitted toward a movable mirror mounted on a precision micrometer translation stage, while the other is reflected toward a fixed aiming mirror. Both mirrors are front-surface aluminized to minimize secondary reflections and were not touched during the experiment to avoid damage.

After reflecting from their respective mirrors, the two beams recombine at the beam splitter. Half of the recombined light is directed toward a viewing screen, where an interference pattern of circular fringes is observed when the optical path lengths of the two arms are nearly equal. The remaining light exits the system through the input optics. Proper alignment of the aiming mirror ensures that the returning beams overlap spatially, producing a centered interference pattern, as illustrated in Figure 1.

The movable mirror is controlled by a micrometer screw mounted on the interferometer arm. One scale division on the screw corresponds to a linear displacement of 1 μm of the mirror, and a full rotation corresponds to a displacement of 50 μm. Since the light travels to the mirror and back, a displacement Δx of the movable mirror produces a change in optical path length of $2\Delta x$. This precise control allows fringe shifts to be counted as the mirror position is varied.

A removable rotation mount is available for inserting optical elements such as a plastic square prism into one arm of the interferometer for index of refraction measurements. The rotation mount is equipped with an angular micrometer that measures angles in degrees and minutes. For temperature-dependent measurements, the movable mirror can be replaced with an aluminum rod whose length changes with temperature. The rod is heated using a variable power supply, and its temperature is monitored using a digital thermometer mounted near the rod.

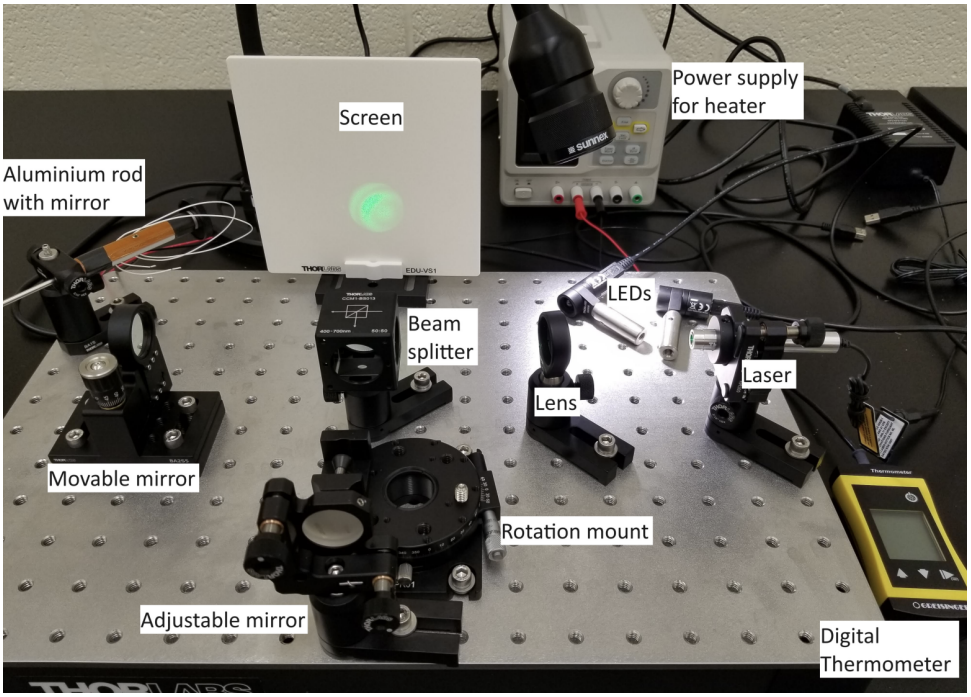

Figure 1: Schematic diagram of the Michelson interferometer used in this experiment.1

2.2 Experimental Procedure

The Michelson interferometer was first aligned using the green laser source. The lens was temporarily removed, and the aiming mirror was adjusted until the two returning beams overlapped. The lens was then replaced and the interference pattern was centered on the screen.

Wavelength of the Green Laser

The movable mirror was adjusted so that the two optical path lengths were approximately equal. The micrometer screw was then rotated in a single direction while counting the number of fringes that appeared or disappeared at the center of the interference pattern. The micrometer readings were recorded and converted to mirror displacements using 1 μm per scale division. Between ten and twenty measurements were taken over as many fringes as could be reliably tracked. The fringe count N was plotted as a function of mirror displacement Δx, and a linear fit was used to determine the laser wavelength.

Index of Refraction

The thickness of the plastic square was measured using a Vernier caliper. The square was placed in the rotation mount and aligned so that the beam was perpendicular to the surface, defining the zero-angle reference. The mount was rotated by small angles while counting fringe shifts. The recorded data were used to determine the index of refraction of the plastic.

Thermal Expansion of Aluminum

The movable mirror was replaced with an aluminum rod, and the interferometer was realigned. The initial temperature was recorded using the digital thermometer. The rod was heated in small increments using a power supply, and the resulting fringe shifts were counted after thermal equilibrium was reached at each temperature. The data were used to determine the coefficient of thermal expansion of aluminum.

3 Data and Analysis

3.1 Wavelengths and Coherence Lengths

The wavelength of the green laser was determined by measuring the number of interference fringes N that appeared or disappeared as the movable mirror was displaced by a distance Δx. Since translating the mirror changes the optical path length by $2\Delta x$, the fringe count satisfies

$$N\lambda = 2\Delta x, \tag{4}$$

implying a linear relationship between N and Δx.

The measured fringe counts were plotted as a function of mirror displacement, and a least-squares linear fit of the form

$$N = m\,\Delta x + b \tag{5}$$

was performed. The resulting best-fit parameters were

$$m = (3.833 \pm 0.054)\ \text{fringes}/\mu\text{m}, \qquad b = (0.11 \pm 0.35)\ \text{fringes}. \tag{6}$$

Using the relation $\lambda = 2/m$, the wavelength of the green laser was found to be

$$\lambda = (521.74 \pm 7.34)\ \text{nm}. \tag{7}$$

The linear fit and corresponding residuals are shown in Figure 2. The coefficient of determination was $R^2 = 0.9986$, indicating excellent linearity. The reduced chi-squared

value was $\chi^2_\nu = 0.398$, consistent with the assigned fringe-count uncertainty of ± 0.5 fringe and suggesting no significant over- or underestimation of measurement errors.

The residuals exhibit no systematic structure and are randomly distributed about zero, indicating that no fringes were missed over the fitted interval. This confirms the validity of the linear model and the reliability of the measured wavelength.

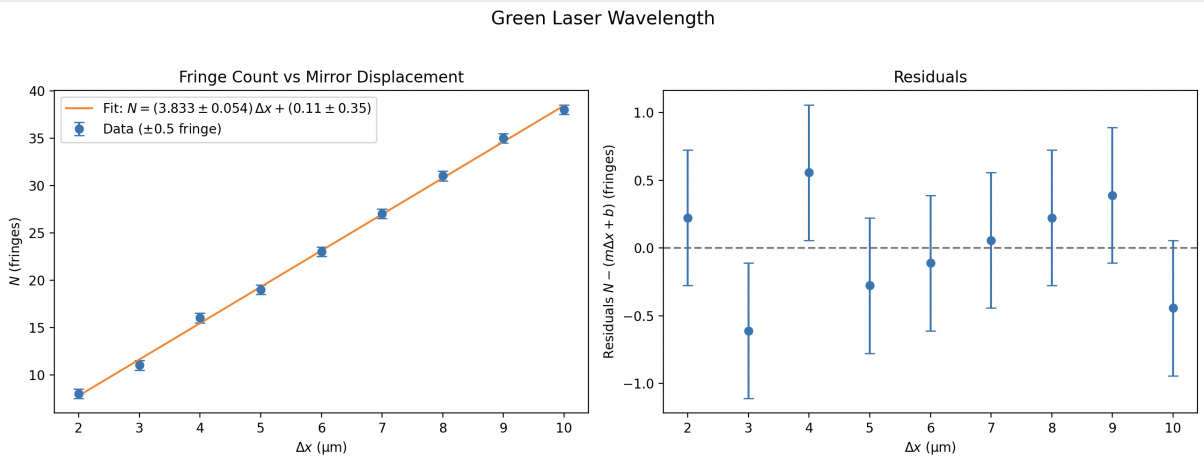

Figure 2: Linear fit of fringe count N versus mirror displacement Δx (left) and corresponding residuals (right) for the green laser wavelength measurement.

Uncertainties could be found in Appendix.

3.2 Index of Refraction

The index of refraction of the plastic square was determined by measuring the number of interference fringes N that appeared or disappeared as the rotation mount was rotated by a small angle θ. The thickness of the plastic was measured using a Vernier caliper to be

$$t = (6.94 \pm 0.01)\,\text{mm}.$$

The angular resolution of the rotation mount was taken to be $\pm 0.5^\circ$, and an uncertainty of ± 0.5 fringe was assigned to each fringe count.

Using the wavelength of the green laser measured previously,

$$\lambda = (521.74 \pm 7.34)\,\text{nm}, \text{Find error propagation in Appendix B}$$

the data were analyzed using the small-angle approximation given in the laboratory manual:

$$N \simeq \frac{t}{\lambda}\,\theta^2 \left(1 - \frac{1}{n}\right), \tag{8}$$

where θ is expressed in radians and n is the index of refraction of the plastic.

Equation (8) predicts a linear relationship between the fringe count N and θ^2. The measured data were therefore plotted as N versus θ^2 and fitted with a least-squares linear model of the form

$$N = m\,\theta^2 + b. \tag{9}$$

The resulting fit yielded

$$m = (4.618 \pm 0.079) \times 10^3\ \text{fringes/rad}^2,$$

with an intercept consistent with zero within uncertainty.

From the fitted slope, the index of refraction was calculated using

$$n = \frac{1}{1 - \dfrac{m\lambda}{t}}, \tag{10}$$

which gave

$$n = 1.532 \pm 0.018.\text{Find error proppgtaion in Appendix C} \tag{11}$$

The linear fit and corresponding residuals are shown in Figure 3. The coefficient of determination was $R^2 = 0.9988$, indicating excellent agreement with the linear model. The reduced chi-squared value was $\chi^2_\nu = 0.311$, consistent with the assigned measurement uncertainties and suggesting no significant systematic error.

The residuals are randomly distributed about zero and show no clear structure, indicating that no fringes were missed during the measurements and that the small-angle approximation is valid over the range of angles used.

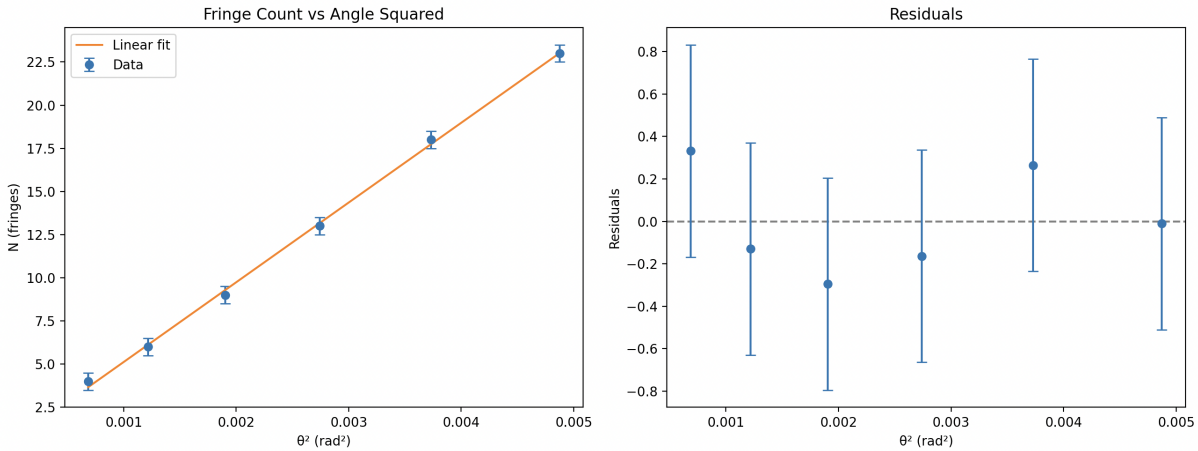

Figure 3: Fringe count N as a function of θ^2 for the plastic square (left) with the corresponding residuals (right).

Uncertainties could be found in Appendix.

3.3 Thermal Expansion of Aluminum

For sufficiently small temperature variations, the expansion is well described by the linearized relationwhere L_0 is the initial length of the rod, λ is the wavelength of the laser, and α is the coefficient of linear thermal expansion.

$$N \simeq \frac{2L_0}{\lambda}\,\alpha\,\Delta T,$$

$$m = \frac{dN}{d(\Delta T)} = \frac{2L_0}{\lambda}\,\alpha.$$

Figure 4 shows the measured fringe count as a function of temperature change together with the linear regression, and residuals plot. The data shows a clear linear trend, and the residuals are randomly distributed about zero with no visible systematic structure, indicating that the linear model is appropriate over the temperature range studied. The

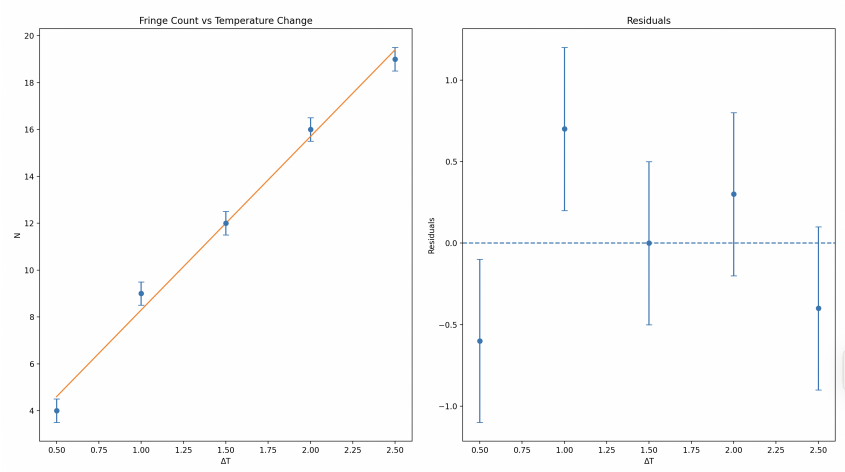

Figure 4: Fringe count N as a function of temperature change ΔT with the best–fit linear regression (left), and residuals of the fit plotted against ΔT (right).

quality of the fit was assessed using the reduced chi–squared and coefficient of determination. The reduced chi–squared value was$\chi^2_{\text{red}} = 1.467$ see the discussion for the reason of high chi–squared value. The coefficient of determination was$R^2 = 0.9920$ showing that the linear model was appropriate and was done well.

The determined slope is:$m = (7.400 \pm 0.383)$ fringes K^{-1} Using the measured rod length $L_0 = 0.09\,\text{m}$ and laser wavelength $\lambda = (521.74\text{nm}$, the coefficient of linear thermal expansion is:

$$\alpha = (2.145 \pm 0.116) \times 10^{-5}\ \text{K}^{-1}.\text{Find error proppgtaion in Appendix D}$$

Uncertainties could be found in Appendix.

4 Discussion and Conclusion

A Michelson interferometer was used to measure the wavelength of a green laser, the index of refraction of a plastic sample, and the coefficient of linear thermal expansion of aluminum through fringe-counting techniques. In all three parts of the experiment, the measured data exhibited strong linear relationships consistent with the theoretical models.

The wavelength measurement showed excellent agreement with the expected value, with a high coefficient of determination and randomly distributed residuals, indicating reliable fringe counting and minimal systematic error. The index of refraction measurement similarly displayed strong linearity between the fringe count and θ^2, validating the small-angle approximation and yielding a value consistent with typical plastics.

For the thermal expansion measurement, a clear linear dependence of fringe count on temperature change was observed. The extracted coefficient of thermal expansion, $\alpha = (2.145 \pm 0.116) \times 10^{-5}\ \text{K}^{-1}$, is consistent with the accepted room-temperature value for aluminum. The reduced chi-squared value indicates reasonable agreement between the data and the linear model within experimental uncertainties.

A notable source of uncertainty in the thermal expansion measurement was the length of the aluminum rod. The rod could not be detached from the mirror assembly, preventing a direct measurement with a Vernier caliper. Consequently, the rod length was assumed

to be $L_0 = 9\,\text{cm}$ as specified in the laboratory manual. This assumption introduces additional uncertainty into the calculation of α, since the thermal expansion coefficient depends linearly on L_0. Despite this limitation, the measured value remains in good agreement with accepted values, demonstrating the effectiveness of interferometry for measuring small thermal expansions.

5 References

- 1- C. Lee, B. Wilson, P. Albanelli, S. Fomichev, and J. Vise, *Interferometry*, University of Toronto Physics Laboratory Manual, current revision 39a6584, July 21, 2025.

Appendix A: Linear Fit Python Code

The following Python script was used to perform the linear least squares analysis, extract the wavelength of the green laser from the fitted slope, and generate the data and residual plots. Other linear regression parameters in the second and third part of the lab was done using the same code with different numbers.

```python
import numpy as np
import matplotlib.pyplot as plt

dx = np.array([2, 3, 4, 5, 6, 7, 8, 9, 10], dtype=float)
Nf = np.array([8, 11, 16, 19, 23, 27, 31, 35, 38], dtype=float)

uN = np.full_like(Nf, 0.5, dtype=float)

x = dx
y = Nf
uy = uN

n = len(x)
sum_x  = np.sum(x)
sum_y  = np.sum(y)
sum_x2 = np.sum(x**2)
sum_xy = np.sum(x*y)
Delta  = n*sum_x2 - (sum_x)**2

m = (n*sum_xy - sum_x*sum_y) / Delta
b = (sum_y*sum_x2 - sum_x*sum_xy) / Delta

residuals = y - (m*x + b)
s2 = np.sum(residuals**2) / (n - 2)
sm = np.sqrt(n * s2 / Delta)
sb = np.sqrt(s2 * sum_x2 / Delta)

chi2 = np.sum((residuals / uy)**2)
dof = n - 2
chi2_red = chi2 / dof
R2 = 1 - np.sum((y - (m*x + b))**2) / np.sum((y - np.mean(y))**2)

lam_um = 2.0 / m
ulam_um = 2.0 * sm / (m**2)
lam_nm = 1000.0 * lam_um
ulam_nm = 1000.0 * ulam_um

print(f"m = {m:.6f} ± {sm:.6f}  [fringes/μm]")
print(f"b = {b:.6f} ± {sb:.6f}  [fringes]")
print(f"λ = {lam_nm:.2f} ± {ulam_nm:.2f}  [nm]")
print(f"Variance s² = {s2:.6f}")
print(f"χ² = {chi2:.3f}, reduced χ² = {chi2_red:.3f}")
print(f"R² = {R2:.6f}")

fig, (ax1, ax2) = plt.subplots(1, 2, figsize=(13, 5))
```

```
46
47  ax1.errorbar(x, y, yerr=uy, fmt='o', capsize=4,
48               label=r'Data ($\pm 0.5$ fringe)')
49  x_fit = np.linspace(x.min(), x.max(), 300)
50  ax1.plot(x_fit, m*x_fit + b, '-',
51           label=rf'Fit: $N = ({m:.3f}\pm{sm:.3f})\,\Delta x +
         ↪  ({b:.2f}\pm{sb:.2f})$')
52  ax1.set_xlabel(r'$\Delta x$ (µm)')
53  ax1.set_ylabel(r'$N$ (fringes)')
54  ax1.set_title('Fringe Count vs Mirror Displacement')
55  ax1.legend()
56
57  ax2.axhline(0, color='gray', linestyle='--')
58  ax2.errorbar(x, residuals, yerr=uy, fmt='o', capsize=4)
59  ax2.set_xlabel(r'$\Delta x$ (µm)')
60  ax2.set_ylabel(r'Residuals $N-(m\Delta x+b)$ (fringes)')
61  ax2.set_title('Residuals')
62
63  plt.suptitle('Green Laser Wavelength', fontsize=14)
64  plt.tight_layout(rect=[0, 0, 1, 0.95])
65  plt.show()
```

Appendix B: Uncertainty Propagation for Wavelength of the Green Laser

$$m = \frac{N}{\Delta x}, \qquad \sigma_N = 1, \qquad \sigma_{\Delta x} = 0.5\ \mu\text{m}$$

$$\sigma_m = \sqrt{\left(\frac{\partial m}{\partial N}\sigma_N\right)^2 + \left(\frac{\partial m}{\partial \Delta x}\sigma_{\Delta x}\right)^2} = \sqrt{\left(\frac{1}{\Delta x}\right)^2 + \left(\frac{N}{\Delta x^2}\,0.5\right)^2} = 0.054\ \text{fringes}/\mu\text{m}$$

$$\lambda = \frac{2}{m}, \qquad \sigma_\lambda = \left|\frac{d\lambda}{dm}\right|\sigma_m = \frac{2}{m^2}\sigma_m$$

$$\lambda = \frac{2}{3.833} = 521.74\ \text{nm}, \qquad \sigma_\lambda = \frac{2}{(3.833)^2}(0.054) = 7.34\ \text{nm}$$

$$\lambda = (521.74 \pm 7.34)\ \text{nm}$$

Appendix C: Uncertainty Propagation for Index of Refraction

$$n = \frac{1}{1 - \dfrac{m\lambda}{t}}, \qquad m = (4.618 \pm 0.079) \times 10^3 \text{ rad}^{-2}, \quad \lambda = (521.74 \pm 7.34) \text{ nm}, \quad t = (6.94 \pm 0.01) \text{ mm}$$

$$n = \frac{1}{1 - \dfrac{(4.618 \times 10^3)(521.74 \times 10^{-9})}{6.94 \times 10^{-3}}} = 1.5318$$

$$\sigma_n^2 = \left(\frac{\partial n}{\partial m}\sigma_m\right)^2 + \left(\frac{\partial n}{\partial \lambda}\sigma_\lambda\right)^2 + \left(\frac{\partial n}{\partial t}\sigma_t\right)^2$$

$$\frac{\partial n}{\partial m} = \frac{\lambda}{t\left(1 - \dfrac{m\lambda}{t}\right)^2}, \qquad \frac{\partial n}{\partial \lambda} = \frac{m}{t\left(1 - \dfrac{m\lambda}{t}\right)^2}, \qquad \frac{\partial n}{\partial t} = -\frac{m\lambda}{t^2\left(1 - \dfrac{m\lambda}{t}\right)^2}$$

$$\sigma_n = \sqrt{\left(\frac{\lambda}{t(1 - \frac{m\lambda}{t})^2}\sigma_m\right)^2 + \left(\frac{m}{t(1 - \frac{m\lambda}{t})^2}\sigma_\lambda\right)^2 + \left(\frac{m\lambda}{t^2(1 - \frac{m\lambda}{t})^2}\sigma_t\right)^2}$$

$$\sigma_n = \sqrt{(0.0139)^2 + (0.0115)^2 + (0.0012)^2} = 0.018$$

$$n = 1.532 \pm 0.018$$

Appendix D: Uncertainty Propagation for Thermal Expansion

$$\alpha = \frac{m\lambda}{2L_0}, \qquad m = (7.400 \pm 0.383) \text{ K}^{-1}, \quad \lambda = (521.74 \pm 7.34) \text{ nm}, \quad L_0 = (0.09 \pm 0.0005) \text{ m}$$

$$\alpha = \frac{(7.400)(521.74 \times 10^{-9})}{2(0.09)} = 2.14493 \times 10^{-5} \text{ K}^{-1}$$

$$\sigma_\alpha^2 = \left(\frac{\partial \alpha}{\partial m}\sigma_m\right)^2 + \left(\frac{\partial \alpha}{\partial \lambda}\sigma_\lambda\right)^2 + \left(\frac{\partial \alpha}{\partial L_0}\sigma_{L_0}\right)^2$$

$$\frac{\partial \alpha}{\partial m} = \frac{\lambda}{2L_0}, \qquad \frac{\partial \alpha}{\partial \lambda} = \frac{m}{2L_0}, \qquad \frac{\partial \alpha}{\partial L_0} = -\frac{m\lambda}{2L_0^2}$$

$$\sigma_\alpha = \sqrt{\left(\frac{\lambda}{2L_0}\sigma_m\right)^2 + \left(\frac{m}{2L_0}\sigma_\lambda\right)^2 + \left(\frac{m\lambda}{2L_0^2}\sigma_{L_0}\right)^2}$$

$$\sigma_\alpha = \sqrt{(1.11015 \times 10^{-6})^2 + (3.01593 \times 10^{-7})^2 + (1.19163 \times 10^{-7})^2} = 1.158 \times 10^{-6} \text{ K}^{-1}$$

$$\alpha = (2.145 \pm 0.116) \times 10^{-5} \text{ K}^{-1}$$